Heliyon 10 (2024) e27449

Contents lists available at ScienceDirect

Heliyon

journal homepage: www.cell.com/heliyon

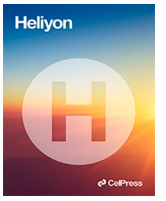

Research article

Coreopsis tinctoria improves energy metabolism in obese hyperglycemic mice

Bingxin Huangfu [a,1], Minglan Yang [a,b,1], Jia Xu [a], Ruxin Gao [a], Yanzhou Hu [a], Yijia Zhao [c], Kunlun Huang [a,c], Xiaoyun He [a,c,*]

[a] *Key Laboratory of Precision Nutrition and Food Quality, Ministry of Education, College of Food Science and Nutritional Engineering, China Agricultural University, Beijing, 100083, China*
[b] *Department of Clinical Nutrition, West China Hospital of Sichuan University, Chengdu, 610041, China*
[c] *Key Laboratory of Safety Assessment of Genetically Modified Organism (Food Safety), The Ministry of Agriculture and Rural Affairs of the PR China, Beijing, 100083, China*

ARTICLE INFO

Keywords:
Coreopsis tinctoria
Obesity
Hyperglycemia
Liver
Kaempferol

ABSTRACT

Coreopsis tinctoria (CT) improves energy metabolism. However, the role of CT in alleviating obesity-induced hyperglycemia by targeting the liver remains unknown. Therefore, this article aims to explore the mechanism by which CT improves energy metabolism and resists hyperglycemia. The water and ethanol extracts of CT were administered to high-fat diet-induced (HFD) obese C57BL/6J mice at a dose of 4 g/kg.bw (low-dose water extract, WL; low-dose ethanol extract, EL) or 10 g/kg.bw (high-dose water extract, WH; high-dose ethanol extract, EH). Mice that consumed a maintenance diet (LFD) were included as blank controls. Network pharmacology, liquid chromatography-mass spectrometry (LC-MS), L02 cell cultivation, and liver transcriptomics were used to examine the mechanism and functional components of CT against obesity-induced hyperglycemia. The results indicated that WL significantly ($p < 0.05$) alleviated glucose intolerance and insulin resistance in obesity-induced hyperglycemia. Kaempferol is the main active compound of CT, which demonstrated significant ($p < 0.05$) anti-hyperglycemic effects in obese mice and L02 cells. Finally, kaempferol significantly ($p < 0.05$; fold change >1.2) shifted the genes involved in carbon metabolism, glycolysis/gluconeogenesis, and the mitogen-activated protein kinase (MAPK) pathways toward the trend of LFD, indicating that it exerts an anti-hyperglycemic effect through these molecular mechanisms. Overall, oral intake of CT lowers blood glucose and improves insulin sensitivity in mice with obesity-induced hyperglycemia. Kaempferol is the primary functional component of CT.

1. Introduction

Obesity and metabolic diseases resulting from excessive energy intake are global public health issues. A meta-analysis showed that the global prevalence of central obesity is approximately 41.5% [1]. Obesity alters lipids, hormones, inflammatory factors, and enzymes, leading to complications such as insulin resistance, type 2 diabetes, dyslipidemia, hyperglycemia, and inflammation [2,3].

* Corresponding author. Key Laboratory of Precision Nutrition and Food Quality, Ministry of Education, College of Food Science and Nutritional Engineering, China Agricultural University, Beijing, 100083, China.
E-mail address: hexiaoyun@cau.edu.cn (X. He).
[1] These authors contributed to this work equally.

https://doi.org/10.1016/j.heliyon.2024.e27449
Received 9 November 2023; Received in revised form 20 January 2024; Accepted 28 February 2024
Available online 8 March 2024

Therapies for obesity and its complications have received significant attention in recent years. Some natural products derived from plants (such as *viburnum stellato-tomentosum*, *ephedra alata*, and *poria cocos*) alleviate obesity and hyperglycemia [4–6]. However, the current research on the impact and mechanism of *Coreopsis tinctoria* on improving hyperglycemia in obese individuals is insufficient.

Coreopsis tinctoria (CT) is a plateau plant native to North America that is widely cultivated in Xinjiang and Yunnan, China [7,8]. CT has a long history of healthcare utilization. Traditional medicine has applied CT to optimize energy metabolism and treat infections and diarrhea [9]. Studies have found that the main active ingredient in CT is flavonoids, and it also contains more than 120 other ingredients, such as polyacetylenes, phenylpropanoids, polysaccharides, and volatile oils [9,10]. As the polarities of these components differ, the composition and content of natural products vary depending on the solvents used for extraction. In *Vivo* and in *Vitro* experiments have shown that CT has biological activities against oxidation, obesity, cancer, aging, hyperglycemia, and hyperlipidemia [11–16]. In exploring the mechanism of CT regulation of glucose and lipid metabolism, existing studies have mainly focused on its down-regulation of proteins related to white adipose differentiation, restoration of pancreatic function, and improvement of intestinal microbes [16–18]. However, limited research has focused on the regulatory effect of CT on liver energy metabolism.

The liver is crucial for energy metabolism. It converts abundant circulating glucose into glycogen and lipids and fuels the body with glycogen and fatty acids during fasting [19]. The glucose and lipid metabolism of the liver is affected by various factors, including nutritional status, cytokines, and hormones. Under conditions of diet-induced obesity and elevated blood glucose levels, accumulation of triglycerides in the liver and crosstalk between the liver and other tissues, result in a decreased ability of the liver to regulate energy balance [20]. Therefore, restoring liver functions at the molecular level is crucial for alleviating metabolic diseases induced by a high-fat diet. Studies have found that CT protects against acute liver injury caused by acrylamide, carbon tetrachloride, and lipopolysaccharide [21–23]. Also, dietary supplementation with CT flower tea while exposed to high-fat diets (HFD) prevents hepatic energy metabolism disorders in rats [24]. Our previous studies found that CT reduces hyperglycemia in obese mice by affecting gut microbiota [25]. Overall, CT can protect the liver, but its effects and mechanisms on the liver in obese-hyperglycemic individuals remain unproven.

To explore the potential of CT in mitigating hyperglycemia and insulin resistance caused by obesity, we examined the effects of CT water extract and ethanol extract on energy metabolism regulation in obese hyperglycemia mice. Also, we studied the mechanism by which CT targets the liver to regulate energy metabolism, as well as the functional components of CT and their mechanisms for alleviating hyperglycemia.

2. Materials and methods

2.1. Extractions of the active ingredients in Coreopsis tinctoria

The *Coreopsis tinctoria* (CT) was harvested in August 2019 from a planting base at an altitude of 3800 m in Saitula, Xinjiang, China. Firstly, it was ground using a high-speed universal grinder (Tianjin Taisite Instrument Co., Ltd). A 60-mesh sieve was used to collect powders with a diameter of less than 0.3 mm. Distilled water and 65% ethanol (E809061, Macklin Co., Ltd) were used as extractants, respectively. The extraction process included sonication, suction filtration, rotary evaporation, and lyophilization. The *Coreopsis tinctoria* powder was extracted three times at a temperature of 80 °C with a solid-liquid ratio of 1:10, and each extraction lasted 45 min [25]. The instrument was purchased from Beijing Earth Long Science and Technology Co., Ltd, Wenling Yangyi Mechanical and Electrical Products Co., Ltd, Beijing Kewei Yongxing Instrument Co., Ltd, and Shanghai Hecheng Instrument Manufacturing Co., Ltd, respectively.

2.2. Explore the impact of Coreopsis tinctoria extract on obese mice

2.2.1. Construction of mouse model and administration of Coreopsis tinctoria extract

4-week-old male C57BL/6J mice, which were specific-pathogen-free, with an initial body weight ranging from 12 to 15 g, were purchased from Beijing Vital River Laboratory Animal Technology Co., Ltd. The mice induced with obesity were fed a 60% high-fat diet (H10060, Beijing HFK Bioscience Co., Ltd.), while the control group of mice was fed maintenance diets (1016706714625204224, Beijing Keao Xieli Feed Co., Ltd.). Four mice were kept in each cage. The mice have free access to food and sterile water. This experiment was conducted in the SPF-grade laboratory of the Superslon & Test Center for Agriculture Product Quality, Ministry of Agriculture (SYXK (Beijing) 2015–0045). The air in the laboratory was exchanged 15 times per hour, and light and dark alternated every 12 h. The mice were observed once a day and weighed weekly.

After one week of adaptive feeding, the mice were assigned to either 60% high-fat diets (HFD) or maintenance diets for 11 weeks. The HFD-induced obese-hyperglycemic mice were selected based on a more than 20% increase in body weight and significantly higher fasting blood glucose levels compared to mice on maintenance diets [26]. The HFD mice were randomly divided into 5 groups (8 mice in each group), and the initial mean body weights were similar. 4 g or 10 g/kg body-weight (.bw) of CT ethanol or water extract was administered to 4 groups of HFD mice every day for 8 weeks, respectively. This dose has been shown to improve energy metabolism in obese mice [25]. Blood biochemistry (liver function, kidney function, and energy metabolism indicators; detailed experimental methods are shown in Section 2.2.4) was used to test the safety at this dose, and the results showed that these doses were non-toxic to mice (supplementary material 1). One group of HFD mice (the HFD group) and the maintenance diet-treated mice (the LFD group) were gavaged with sterile water. This experiment was approved by the Animal Ethics Committee of China Agricultural University (Approval number: KY1700038).

2.2.2. Insulin and glucose tolerance test

An insulin tolerance test (ITT) was conducted in the 4th week of gavage. The mice were fasted for 4 h and injected intraperitoneally with 0.7 U/kg.bw insulin (NovoRapid® Penfill®, Novo Nordisk Co., Ltd.) [27,28]. The mice had their plasma glucose (PG) levels measured at 0, 15, 30, 45, and 60 min after injection. A glucose tolerance test (GTT) was conducted in the fifth week. The mice were fasted for 16 h and injected intraperitoneally with 1.5 g/kg.bw glucose (50-99-7, Sigma-Aldrich Co., Ltd.) [29–31]. The blood glucose level of each mouse was measured at 0 min, 15 min, 30 min, 45 min, 60 min, and 120 min after the injection. The ITT and GTT results were quantified by calculating the area under the curve (AUC) using the following formula: Duration * ($PG_{0\ min} + PG_{15\ min}$)/2 + duration * ($PG_{n\text{-}1\ min} + PG\ n_{min}$)/2 [32].

2.2.3. Detection of energy metabolism and obese hyperglycemia development

After 7 weeks of gavage, the mice's respiratory oxygen consumption was measured for 24 h using a Panlab Harvard Apparatus 10 Cage Respiratory Metabolism System. The data was processed by Metabolism Version 3.0. In the final week of the experiment, the mice were subjected to cold stimulation at 4 °C for 4 h, and their core temperature was measured with a rectal thermometer. Finally, mice were weighed and sacrificed by cervical dislocation after a 16-h fasting period. Finally, the mice were sacrificed by cervical dislocation. Liver, subcutaneous fat (SUB), and epididymal fat (EP) were collected. The organ coefficient was calculated as the proportion of organ weight to fasting body weight.

2.2.4. Serum biochemical analysis

Blood was collected when the mice were sacrificed and serum was obtained by centrifugation. Serum insulin levels were measured using an insulin ELISA kit (HY-10069, Beijing Huaying Biotechnology). Blood was collected when sacrificed the mice and serum was obtained by centrifugation. The Hitachi 7600–020 automatic biochemical analyzer was used to detect the levels of serum biochemical indicators. The high-density lipoprotein (HDL, 1000020238), low-density lipoprotein (LDL, 1000020248), triglycerides (TG, 1000020090), cholesterol (CHO, 1000020080), alkaline phosphatase (ALP, 1000020020), aspartate aminotransferase (AST, 1000020010), alanine aminotransferase (ALT, 1000020000), total protein (TP, 1000020140), albumin (ALB, 1000020150), uric acid (UA, 1000020070), creatinine (CREA, 1000020170), and glucose (GLU, 1000020100). The kits were purchased from Zhongsheng Beikong Biotechnology Co., Ltd.The blood urea nitrogen (BUN, BC1530) kits were purchased from Solarbio Life Science Co., Ltd. and all procedures were conducted following the instructions provided in the instructions in the manual.

2.3. Identification of active ingredients in Coreopsis tinctoria

2.3.1. Composition analysis

Liquid chromatography-mass spectrometry (LC-MS, TripleTOF5600+, AB SCIEX™) was used to detect and compare the components of CT's water extract and ethanol extract. The water and ethanol extracts were pre-treated by ultrasonication in a water-ice bath and then centrifuged to obtain the supernatant for liquid-phase detection. In liquid chromatography-mass spectrometry, the chromatographic column used is the SHIMADZU InerSustain C18 (100 × 2.1 mm, 2 μm). The column temperature was 35 °C. The flow rate is 0.300 mL/min. The mobile phase is A.Equate = "acetonitrile", B.Equate = "0.1% CH3COOH–H2O". The chromatographic conditions are as follows: 0 min (A:0% B:100%), 10 min (A:50% B:50%), 13 min (A:95% B:5%), 14 min (A:0% B:100 %), and 15 min (A:0% B:100%); the mass spectrometry conditions include a scan range of *m/z* 100–1500, DIA for the scan mode, a capillary voltage of 5000 V (positive) and a 4500 V (negative), a capillary temperature of 500 °C(DP: 60V, CE: 35V, CES: 15V). The LC-MS raw data was imported into MS-DIAL 3.82 software for preprocessing, and the extracted peak information was compared with the MassBank, Respect, and GNPS (14,951 records in total) databases. Overall, the outputs include sample information, retention time, mass-to-nucleus ratio, and mass spectral response intensity (peak area).

2.3.2. Network pharmacology

The bioactive substances in CT were identified by screening the compounds detected by LC-MS using the Traditional Chinese Medicine Systems Pharmacology Database and Analysis Platform (TCMSP) based on oral bioavailability (OB) ≥ 30% and drug-likeness (DL) ≥ 0.18. The protein targets in the human body affected by the bioactive substances in CT were distinguished using the PharmMapper database (norm fit ≥0.7). Subsequently, the target proteins were converted into gene names using the UniProt database. Obesity, hyperglycemia, insulin resistance, and diabetes-related targets were searched in the DisGeNET database. Bioinformatics was used to identify the intersection between CT and disease-associated targets.

The protein-protein interaction (PPI) was constructed using the STRING 11.0 database, and the Cytoscape 3.8.2 software was used to analyze the network. The critical target protein for CT to alleviate obesity-induced hyperglycemia is screened with the closeness centrality and betweenness centrality greater than the median and the degree value (degree) greater than 2 times the median. Bioinformatics was used for the enrichment analysis of biological processes (BP), cellular components (CC), and molecular functions (MF) in terms of GO (Gene Ontology) function and KEGG (Kyoto Encyclopedia of Genes and Genomes) pathway enrichment analysis. Finally, the Cytoscape 3.8.2 software was used to visually analyze the relationship between active ingredients and disease targets in CT. Molecular docking was performed using the CB-Dock online platform to identify combinations with a binding activity (affinity less than −7.0 kcal mol^{-1}) [33].

2.3.3. In vitro verification of active ingredients against obese-induced hyperglycemia

Hepatic L02 cells were obtained from China Agricultural University. L02 is a normal human hepatocyte cell line, which better

reflects energy metabolism in humans [34]. The cells were cultured at 37 °C with 5% CO_2. 300 μM sodium palmitate (PA, P799157, Macklin Co., Ltd) was used to induce insulin resistance in L02 cells [35,36]. This concentration of PA significantly reduced glucose consumption in L02 cells, as measured by the Glucose Oxidase Assay Kit (E1011, Applygen Co., Ltd.). However, it did not affect cell viability, as measured by the Enhanced CCK-8 Kit (C0037, Beyotime Biotechnology Co., Ltd.). The flavonoid substances of CT identified in 2.3.2 (kaempferol, taxifolin, eriodictyol, luteolin) were administered to insulin-resistant L02 cells at concentrations of 0, 1.5625, 3.125, 6.25, 12.5, 25, 50, and 100 μM for 24 h, respectively. The purity of the flavonoid substances are greater than 98% (HPLC grade), and were purchased from Solarbio Life Science Co., Ltd (SK8030, SL8300, YZ1359S, amd SE8200). The Glucose Oxidase Assay Kit was used to determine the improvement in glucose consumption caused by the flavonoid compounds. These flavonoids were dissolved in a 0.05% Dimethyl Sulfoxide (DMSO, D8371, Solarbio Life Science Co., Ltd.) solution. To eliminate the influence of DMSO on the experiment, a PA control group was established in which the cells were treated with a 0.05% DMSO solution.

2.3.4. In vivo transcriptomics of verification anti-hyperglycemic mechanism

4-week-old male C57BL/6J mice of SPF grade were used as experimental animals. The feeding method is the same as described in Section 2.2.1. Our previous results showed that WL and its main active ingredient (kaempferol, KL) showed promising hypoglycemic effects. We then constructed an obese hyperglycemic mouse model and provided them with WL and KL, respectively. The obese hyperglycemic mice were obtained by feeding a 45% high-fat and 35% carbohydrates diet (H10045, Beijing HFK Bioscience Co., Ltd.) for 10 weeks [37,38]. The inclusion criteria for HFD-induced obese-hyperglycemic mice were identical to those described in section 2.2.1, ensuring the reliability and reproducibility of the findings [26]. The obese hyperglycemic mice were treated with 4 g/kg.bw of CT water extract or 25 mg/kg.bw of kaempferol (IK0020, Solarbio Life Science Co., Ltd.) for 8 weeks. 5 mice were arranged into each group.

After sacrificing mice, total RNA was extracted from liver tissue using the Trizol method. The RNA was sequenced on the Illumina platform, and the transcriptome mRNA sequencing mode was paired-end 150bp (PE50). Reference genome alignments were performed using Cutadapt (v1.10), Tophat2 (v2.0.13), Cufflinks (v2.2.1), Cuffnorm, and Cuffdiff. Differentially expressed gene analysis, GO functional enrichment analysis, and KEGG pathway analysis were performed [39,40]. Finally, Venny 2.1.0 was used to visualize the significantly changed genes between WL and KL compared to HFD. Lingbo MicroClass was used to complete principal component analysis (PCA) and visualize the fold difference (log_2) comparison between LFD and HFD versus KL and HFD.

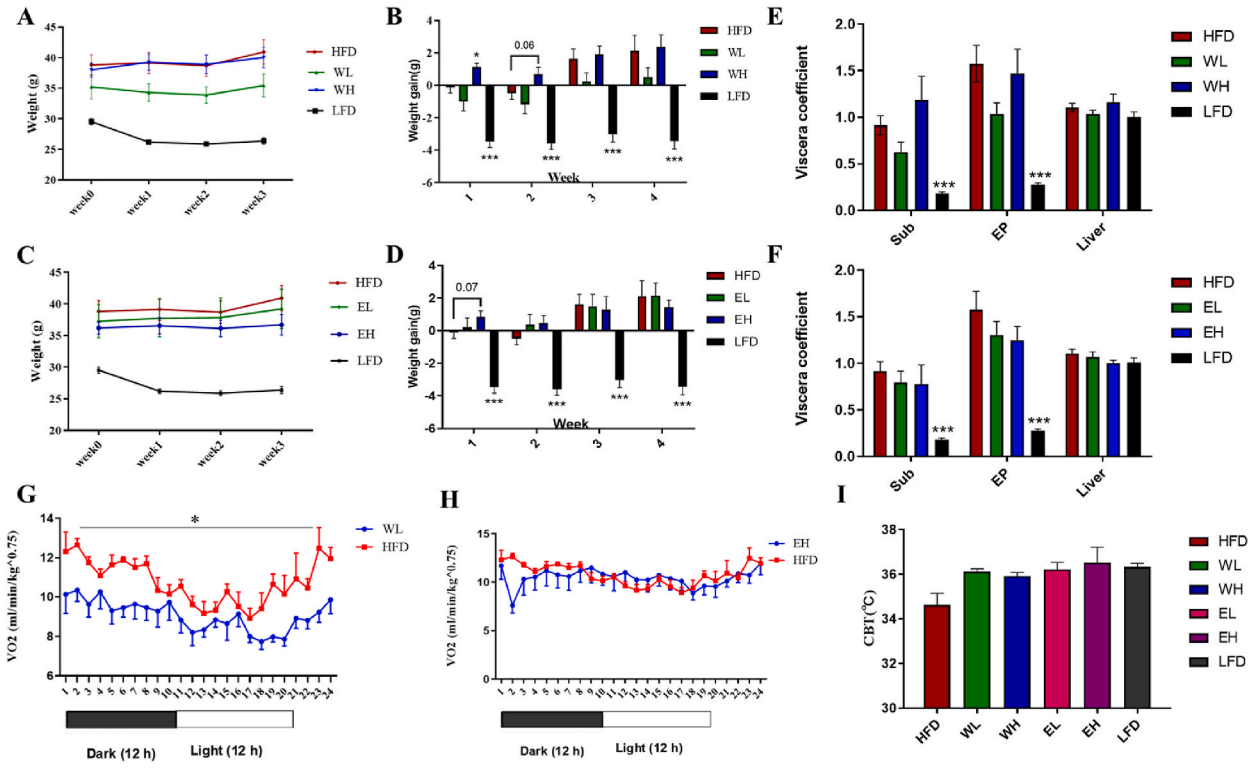

Fig. 1. The Anti-obesity effect of *Coreopsis tinctoria* in HFD hyperglycemic mice. (A) Weight change after CT water extract treatment; (B) weight gain after CT water extract treatment; (C) weight change after CT ethanol extract treatment; (D) weight gain after CT ethanol extract treatment; (E) organ coefficient of CT water extract-treated mice; (F)organ coefficient of CT ethanol extract-treated mice; (G) oxygen consumption after WL treatment (H) oxygen consumption after EH treatment (I) core body temperature after cold stimulation.

2.4. Data analysis

Office 2019 Excel software was used for data calculation, and the results were expressed as the mean ± standard deviation (SD). One-way analysis of variance was used to calculate the significant differences between groups in transcriptomic analysis, with Tukey analysis as a post-hoc test. The Student's *t-test* was used to calculate the significant difference between groups in other analyses. Graphing was performed using the GraphPad Prism 8 software package and BioMicroClass.

3. Results

3.1. Coreopsis tinctoria improves energy metabolism in HFD mice

The low dose (4 g/kg.bw) water extract (WL), high dose (10 g/kg.bw) water extract (WH), low dose (4 g/kg.bw) ethanol extract (EL), and high dose (10 g/kg.bw) ethanol extract (EH) of *Coreopsis tinctoria* (CT) inhibited the body weight gain of HFD mice. Although no significant difference was observed between the mice treated with CT extract and those on an HFD in the first four weeks of gavage, there are downward trends that can be observed. In the fourth week, the average body weight of mice treated with WL was 76.51% lower than that of the HFD group, while the average body weight of mice treated with EH was 31.54% lower than that of the HFD group (Fig. 1A–D). Also, although CT treatments did not significantly reduce the visceral coefficient of white adipose (SUB and EP) and liver organs in mice, WL and EH lowered these indicators by 32.50% , 35.22% , 6.42%, and 15.86%, 21.08%, 9.22% compared with those of the HFD mice, respectively. These results indicated that WL and EH had a slight reversing effect on the obesity of HFD mice (Fig. 1E–F).

In contrast to WH and EL, WL and EH treatments showed better performance in improving obesity. Therefore, the oxygen consumption (which reflects metabolic rate) of these two groups of mice in both light and dark environments was measured and compared with that of HFD-treated mice. The results showed that WL treatment significantly ($P < 0.05$) increased the oxygen consumption and energy metabolism levels of HFD mice (Fig. 1G). However, EH treatment did not significantly impact oxygen consumption in HFD mice (Fig. 1H). Moreover, the rectal temperature test results showed that WL, WH, EL, and EH treatments prevented the decrease in core temperature among HFD mice during cold stimulation (Fig. 1I), indicating that CT treatment increased energy utilization in the HFD mice.

LFD represents the mice that ingested maintenance feed and were gavaged with sterile water; HFD represents the mice that ingested HFD and were gavaged with sterile water; WL represents the mice that ingested HFD and were gavaged with 4 g/kg.bw CT water extracts Mice; WH represents mice that ingested HFD and were gavaged with 10 g/kg.bw CT water extract; EL represents mice that ingested HFD and were gavaged with 4 g/kg.bw CT ethanol extract; EH represents mice that ingested HFD and were gavaged with 10 g/kg.bw CT ethanol extract. The body weight and viscera coefficient of the mice were measured during and after the experiment, respectively (n = 7–8). Oxygen consumption was measured after 7 weeks of treatment (n = 4). Core body temperature (n = 4). The results were expressed as mean ± SD. The Student's t-test was used to calculate the significance of each group compared to the HFD group. * indicates $p < 0.05$; ** indicates $p < 0.01$; *** indicates $p < 0.001$.

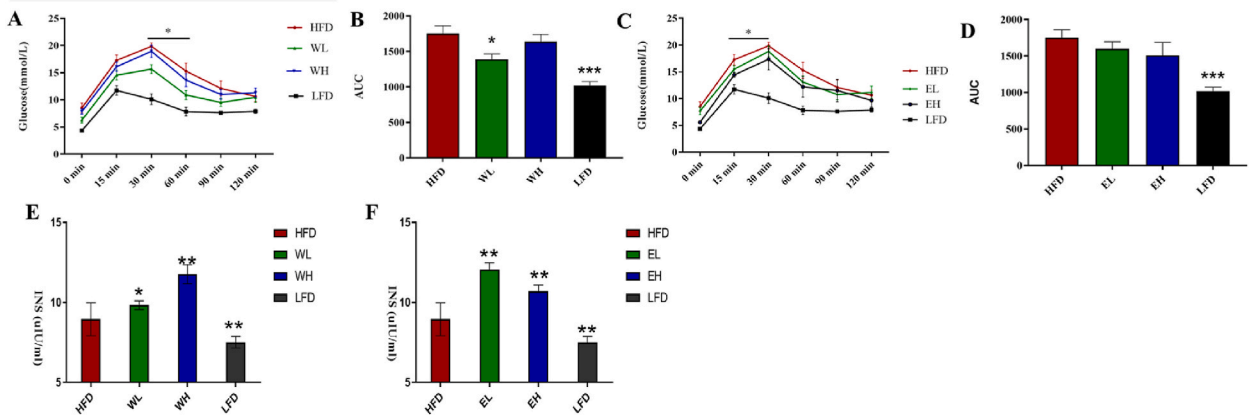

Fig. 2. ***Coreopsis tinctoria*** **improves GTT and increased the insulin levels of HFD mice** (A) water extract GTT (B) area under water extract GTT curve (C) ethanol extract GTT (D) area under ethanol extract GTT curve (E) plasma insulin levels of water extract-treated mice (F) plasma insulin levels of ethanol extract-treated mice. GTT was performed on the 5th week of the experiment. Serum insulin levels were measured when the mice were sacrificed in the 8th week. The GTT results were quantified by calculating the AUC. The results were expressed as mean ± SD (n = 7–8). The Student's t-test was used to calculate the significance of each group compared to the HFD group. The results were expressed as mean ± SD. * indicates $p < 0.05$; ** indicates $p < 0.01$; *** indicates $p < 0.001$.

3.2. CT improves glucose metabolism and insulin resistance in HFD mice

As shown in Fig. 2A–B, WL treatment significantly decreased the AUC of HFD-induced obesity in mice ($P < 0.05$), indicating that WL has the potential to restore impaired glucose tolerance. In contrast, the WH, EL, and EH treatments slightly decreased the AUC compared to the HFD group (Fig. 2A–D). WL has also been found to improve insulin tolerance (Supplementary Material 3). Also, WL, WH, EL, and EH significantly ($P < 0.05$) increased serum insulin levels (Fig. 2E–F).

3.3. Network pharmacology prediction of the mechanism of CT in reversing obesity-induced hyperglycemia

The LC-MS analysis revealed over 100 components in the water and ethanol extracts of CT. The lists of critical components and the profile results of total ion chromatograms are displayed in supplementary material 2 (Table S2 and Fig. S2, respectively). Out of these components, 6 active ones were identified after screening for OB $\geq$ 30% and DL $\geq$ 0.18 (Table 1). These protein targets were converted into 91 corresponding genes (Fig. 3A).

In addition to obesity and hyperglycemia, overnutrition is often accompanied by insulin resistance and diabetes, and these diseases further hinder cells from effectively utilizing glucose [41]. Therefore, the shared target genes of CT with obesity, diabetes, hyperglycemia, and insulin resistance were calculated. The results showed that CT has 57, 44, 27, and 6 shared genes with obesity (2.02%), diabetes (1.87%), hyperglycemia (2.46%), and insulin resistance (3.70%), respectively (Fig. 3A). Prediction results suggest that CT has the potential to target these diseases.

Cytoscape 3.8.2 was used to quantify the PPI network obtained from the String database. It reflects the interactions among the target proteins of CT shared with the four diseases (Fig. 3B). The larger the node and the redder the color, the higher the association frequency between the gene and other nodes. Critical target genes were identified based on network topology parameters, which included betweenness centrality (>0.0247), closeness centrality (>0.5333), and degree (>16). We found that Albumin (ALB), epidermal growth factor receptor (EGFR), estrogen receptor 1 (ESR1), human heat shock protein 90 kDa alpha (HSP90AA1), SRC proto-oncogene, non-receptor tyrosine kinase (SRC), and kinase insert domain receptor (KDR) have a high node association frequency, association tightness, and communication function in protein interaction, which means they play critical roles in CT intervention of hyperglycemia. Furthermore, the KEGG enrichment showed that CT acts on the FoxO signaling pathway, endocrine resistance, and estrogen signaling pathway (Fig. 3C). GO enrichment analysis showed that CT interfered with the cellular response to hormones and reactive oxygen species at the biological process level (Fig. 3D). Also, it mainly regulates cellular components such as vesicle lumen, ficolin-1-rich granule, and ficolin-1-rich granule lumen. The active ingredients are predicted to regulate molecular functions through ATPase binding, nuclear receptor activity, and steroid binding. Based on the chemical properties of the active compound in CT, flavonoids are the primary functional substances (Fig. 3E).

Functional substances detected from CT extracts included kaempferol, taxifolin, eriodictyol, luteolin, aloe-emodin, and quercetin. The intersection targets of these substances with obesity, hyperglycemia, insulin resistance, and diabetes were calculated and analyzed.

3.4. Anti-hyperglycemic composition of Coreopsis tinctoria

To identify the key flavonoids in CT that improve hepatic glucose metabolism in individuals with excess energy, in Vitro experiments were conducted using the L02 cell line. This experiment focused on the effects of functional flavonoids (kaempferol, taxifolin, eriodictyol, luteolin) in the water extract of CT on the glucose consumption and viability of PA-treated L02 cells. The results showed that kaempferol at the dose of 50–100 μM significantly ($P < 0.05$) improved impaired glucose consumption (Fig. 4B) caused by PA treatment of L02 cells and maintained the growth of L02 cells (Fig. 4J). However, taxifolin, eriodictyol, and luteolin did not improve the impaired glucose consumption caused by PA treatment (Fig. 4). Thus, kaempferol is a promising anti-hyperglycemic substance in CT and is safe for liver cells. It was further verified in Vivo in the following experiment.

3.5. In vivo anti-hyperglycemic property of CT and kaempferol

After being treated with 4 g/kg.bw of CT water extract (WL) or 25 mg/kg.bw of kaempferol (KL) for 8 weeks, blood glucose levels in obese hyperglycemic mice were reduced ($p = 0.06$ and $p < 0.01$, respectively, Fig. 5A). Compared to obese hyperglycemic mice, WL treatment significantly altered the expression of 1448 genes in the mouse liver, while KL treatment significantly altered the expression

Table 1
Six active compounds in *Coreopsis tinctoria*.

Detected In	Active Component	OB (%)	DL
Water & Alcohol extract	kaempferol	41.88	0.24
Water & Alcohol extract	taxifolin	57.84	0.27
Water & Alcohol extract	eriodictyol	71.79	0.24
Water & Alcohol extract	luteolin	36.16	0.25
Alcohol extract	aloe-emodin	83.38	0.24
Alcohol extract	quercetin	46.43	0.28

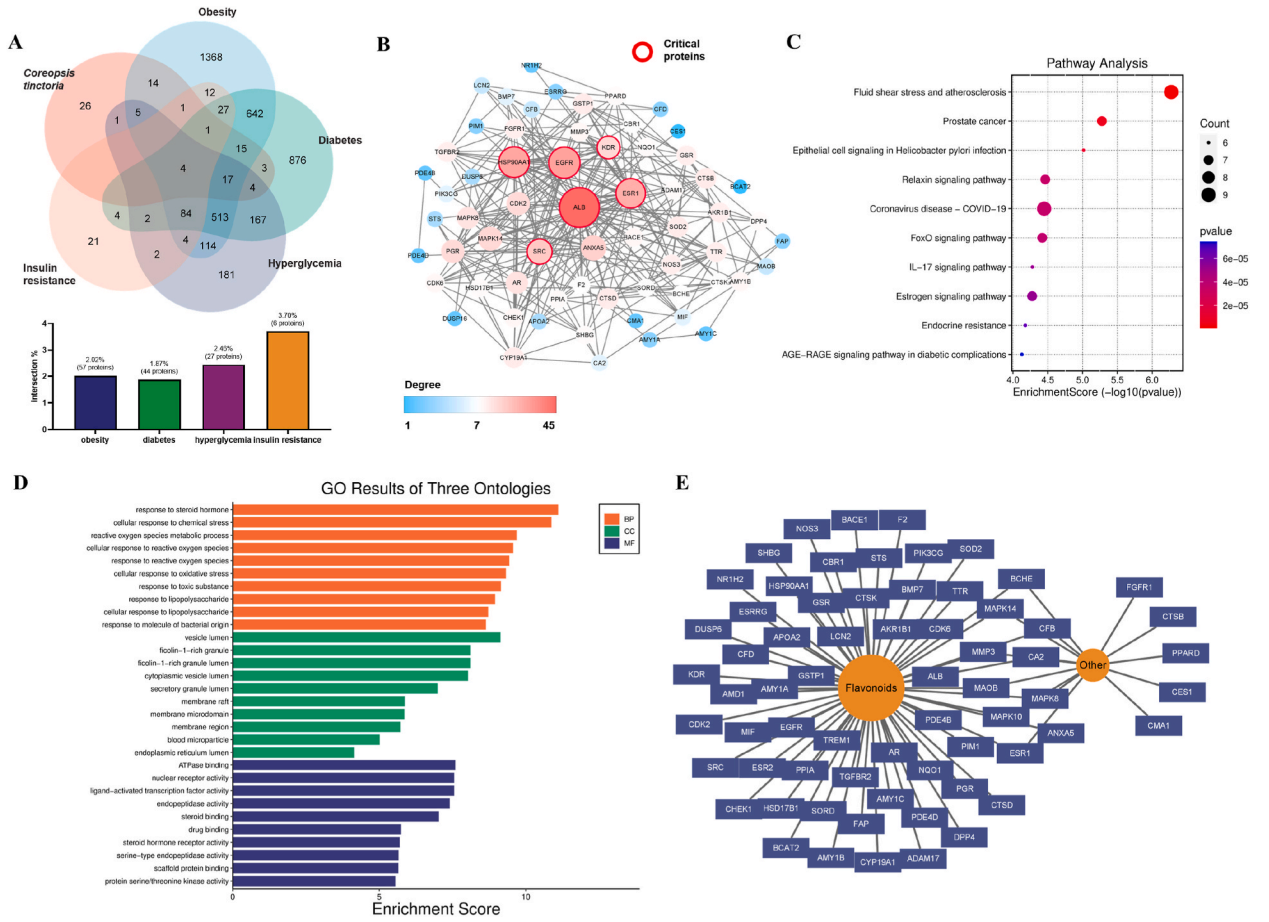

Fig. 3. Prediction of the mechanism of *Coreopsis tinctoria* on alleviating hyperglycemia caused by obesity by Network pharmacology (A) Venn diagram of functional components in Coreopsis tinctoria and disease targets (B) PPI network diagram (C) KEGG enrichment (D) GO enrichment—biological process, cellular component, molecular function (E) correspondence between functional components and intervention targets.

of 977 genes (Fig. 5B). 400 of these genes overlap and corroborate that KL is the critical active ingredient in the water extract of CT. Partial least squares-discriminant analysis (PLS-DA) showed that the RNA levels in the livers of mice treated with WL or KL deviated from those of mice on HFD and shifted towards the mice on LFD (Fig. 5C).

The KEGG enrichment analysis showed that WL impacted several signal pathways, including thermogenesis, non-alcoholic fatty liver disease (NAFLD), steroid hormone biosynthesis, retinol metabolism, PPAR signaling pathway, bile secretion, and primary bile acid biosynthesis (Fig. 5D). Differential genes between HFD and KL-treated mice were found to be enriched in MAPK signaling pathway, steroid hormone biosynthesis, retinol metabolism, carbon metabolism, glucagon signaling pathway, PPAR signaling pathway, AGE-RAGE signaling pathway in diabetic, and glycolysis/gluconeogenesis signaling pathways (Fig. 5E). Among the pathways, the carbon metabolism, glycolysis/gluconeogenesis, and MAPK signaling pathways are directly related to liver glucose metabolism. Compared to the HFD group, the significantly altered genes enriched in these pathways by KL administration shifted towards those of the LFD group, indicating that KL improved hyperglycemia caused by HFD through these signaling pathways (Fig. 5F).

Using PPI and molecular docking, we simulated interactions between proteins identified in Fig. 5F and the possibility of KL binding to these proteins at the protein level (Fig. 5G). The size of the protein node in Fig. 5G corresponds to their interactions with other proteins. Pyruvate kinase L/R (PKLR) is the most critical protein in the network and participates in two signaling pathways: carbon metabolism and glycolysis/gluconeogenesis. The results of molecular docking affinity analysis revealed that KL can bind to multiple target proteins. An affinity score that is below −7 kcal mol^{-1} (marked in red) indicates that the binding potential is high, while a score greater than −7 kcal mol^{-1} (marked in blue) suggests a low binding potential. The serine dehydratase like (SDSL) protein, which is specific to type 2 diabetes and mellitus, showed the best affinity score of −9.4 kcal mol^{-1} among all the proteins analyzed [42]. The molecular docking diagram of PKLR and SDSL proteins with KL is shown in Fig. 5H.

For Fig. 5A, the results were expressed as mean ± SD. * means a significant difference ($p < 0.05$) compared with the HFD group. In transcriptomics, significantly changed genes were identified using a p-value of less than 0.05 (determined through one-way ANOVA) and a fold change greater than 2. All pathways enriched by KEGG (WL and KL) and enriched by GO are presented in Supplementary Material 4.

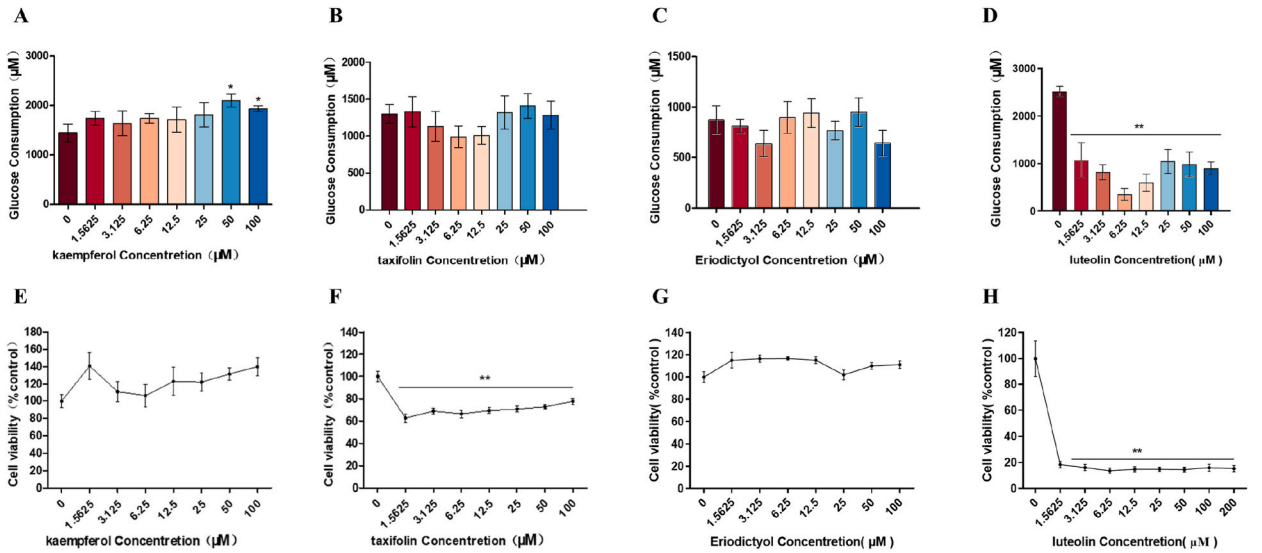

Fig. 4. Effects of *Coreopsis tinctoria* flavonoids on glucose consumption and cell viability in L02 cells (A–D) Glucose consumption after flavonoids treatment (E–H) Cell viability after flavonoids treatment 0.05% DMSO solution was used as the solvent. The DMSO solution at this dose did not affect the glucose consumption and cell viability of L02 cells. 0.05% DMSO was added to the control group to eliminate errors. The results (n = 6) were expressed as mean ± SD. The Student's t-test was used to calculate the significance of the difference between the groups treated with flavonoids and those that did not receive flavonoid treatment. The results were expressed as mean ± SD. * indicates $p < 0.05$; ** indicates $p < 0.01$; *** indicates $p < 0.001$.

4. Discussion

Obesity, which can be caused by excessive energy intake, is often accompanied by increased adipose tissue, abnormal chemokines, adipokines, and pro-inflammatory cytokines [43]. These indicators lead to decreased insulin sensitivity, an inability to suppress glucose output from the liver, and impaired glucose utilization by cells [44]. In individuals with insulin resistance, cellular glucose transport is reduced, and plasma fatty acids and glucose levels are elevated [35,45]. Our results found that the water and alcoholic extracts of CT slightly reduced the body weight and the proportion of white adipose in HFD mice. Furthermore, the water and ethanol extracts of CT improved GTT and ITT in HFD mice. Among them, the water extract of CT at a dose of 4 g/kg.bw (WL) showed the best recovery effect on insulin sensitivity with a significant difference compared to the HFD group. Studies have shown that insulin resistance, accompanied by insufficient insulin secretion caused by damage to pancreatic β cells, results in type 2 diabetes [45]. The serum insulin levels of HFD mice were significantly increased after the administration of CT extract, suggesting that CT extract can prevent the development of type 2 diabetes in obese individuals. Literature has confirmed that CT regulates insulin production by improving pancreatic inflammation and reducing damage in obese individuals [13,46,47]. Under a high-fat diet, the body takes in excess energy, which leads to a physiological imbalance in energy consumption [48]. Previous studies have confirmed that increasing energy expenditure improves obesity and insulin sensitivity [49–51]. We found that administration of 4 g/kg.bw CT water extract increased the mice's oxygen consumption, indicating that CT increased metabolic expenditure compared to the HFD mice [52].

Network pharmacology aims to predict biologically active natural products in plants and their molecular mechanisms by analyzing the relationship among components, targets, and pathways [53]. Our prediction results indicated that the bioactive natural products (kaempferol, taxifolin, eriodictyol, luteolin, aloe-emodin, and quercetin) in CT act on the FoxO signaling pathway, endocrine resistance, and estrogen signaling pathways. The PI3K/AKT signaling pathway negatively regulates FoxO transcription factors, and the activation of FoxO transcription factors in the liver triggers hyperglycemia [54,55]; endocrine resistance leads to an imbalance between insulin secretion and sensitivity in target tissues, causing metabolic dysregulation and elevated blood sugar [56]. Estrogen signaling pathways regulate glucose metabolism through downstream pathways, including glucose transporter receptor α and insulin release [57,58]. ALB, EGFR, ESR1, HSP90AA1, SRC, and KDR are critical targets of CT. The HSP90 family and SRC contribute to insulin resistance, which interacts with the endocrine resistance signaling pathway [59,60]. EGFR and ESR1 are closely related to the estrogen signaling pathway and regulate energy metabolism [61]. Furthermore, CT water extracts regulated the steroid hormone biosynthesis pathway in the mouse life, which was consistent with the estrogen signaling pathway predicted by network pharmacology. In addition, CT water extract acts on the non-alcoholic fatty liver disease and PPAR signaling pathways. These pathways are related to insulin resistance and energy metabolism in response to excess nutrition [62,63]. These findings suggest that improved energy metabolism under overnutrition is a potential mechanism by which CT alleviates hyperglycemia.

Network pharmacology showed that the main active ingredient of CT in lowering blood sugar is flavonoids. The CT water extract contains bioactive flavonoids such as kaempferol, taxifolin, eriodictyol, and luteolin. The impact of these flavonoids on cellular glucose uptake under nutrient overload was verified in the L02 cell line. Elevated glucose uptake increases the utilization of energy by liver

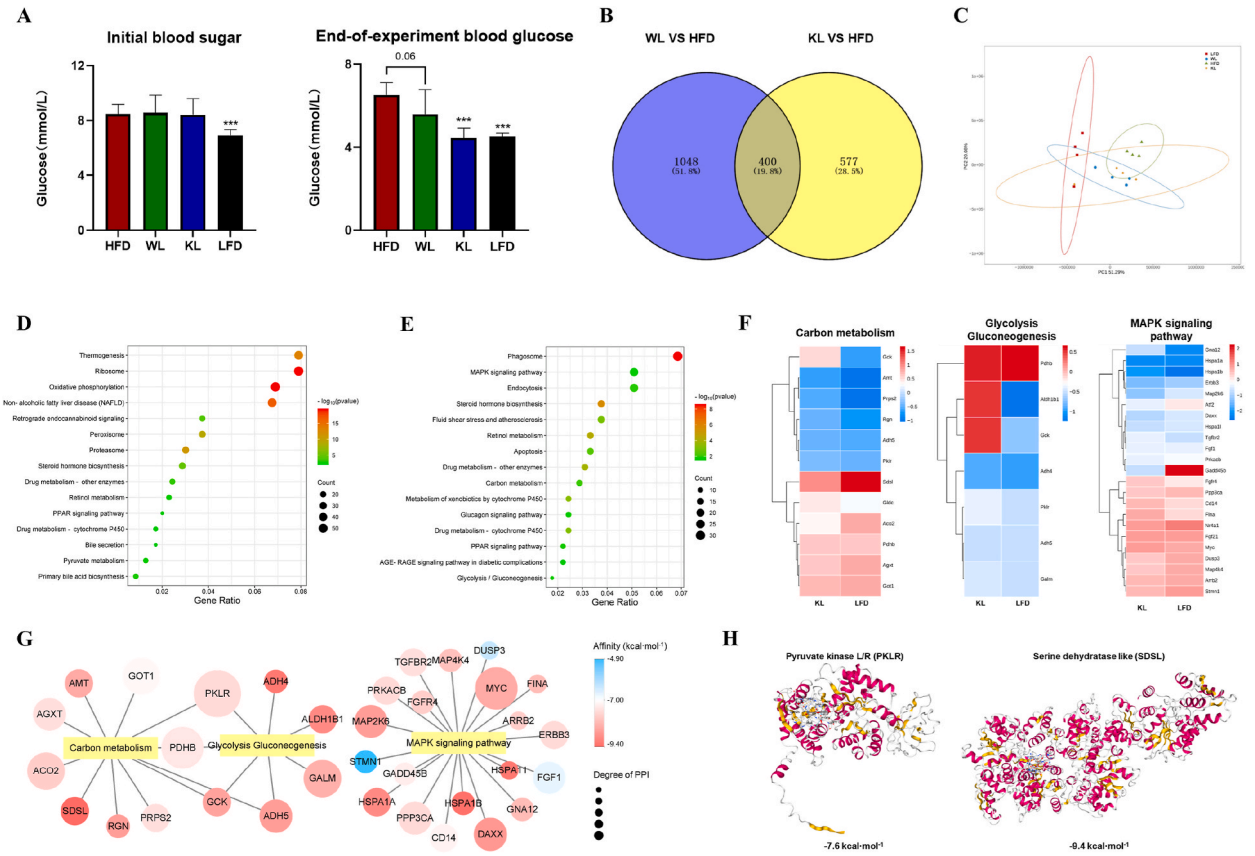

Fig. 5. Validation of Coreopsis tinctoria and kaempferol in alleviating obese-hyperglycemia based on liver transcriptomics (A)Alleviating effects of WL and KL treatments on high-fat diet-induced hyperglycemia (B) Venn diagram of genes altered in WL and KL compared to HFD (C) Partial least squares-discriminant analysis (PLS-DA) analysis (D) WL VS HFD KEGG enrichment (E) KL VS HFD KEGG enrichment (F) Heat-map of KL-altered genes in carbon metabolism, glycolysis/gluconeogenesis, and MAPK signaling pathways (G) Protein interaction and molecular docking (with KL) of differential genes enriched in carbon metabolism, glycolysis/gluconeogenesis, and MAPK signaling pathways (H) The molecular docking of PKLR and SDSL proteins with KL.

cells, glycogen production, and insulin sensitivity, thereby reducing the excess of glucose in the circulation [64,65]. The results showed that the flavonoid kaempferol in CT significantly promoted glucose uptake in L02 cells under PA stimulation. It was shown that CT improved the homeostasis of liver glucose metabolism under conditions of excess energy, and kaempferol was identified as the main functional component in CT. Transcriptomics analysis revealed that treatment with KL (25 mg/kg.bw kaempferol) in HFD mice intervened in the clustering of genes in the liver. Furthermore, KL treatment restores carbon metabolism, glycolysis/gluconeogenesis, and MAPK signaling pathways in the liver of obese hyperglycemic mice to levels similar to mice on LFD. These pathways are directly related to liver glucose metabolism. Carbon metabolism and glycolysis/gluconeogenesis signaling pathways are responsible for regulating the glucose storage and release of the liver, playing a crucial role in maintaining blood glucose homeostasis [66–68]. The MAPK signaling pathway connects extracellular stimuli with intracellular signaling and is crucial in glucose homeostasis and thermogenesis [69]. Among these signaling pathways, PKLR and SDSL are predicted to be potential protein targets for KL. Overall, oral administration of KL alleviates obesity-induced hyperglycemia by restoring the signaling pathways against HFD.

This article explores the mechanism by which CT improves hyperglycemia and insulin sensitivity for the first time at the transcription level, using network pharmacology analysis and examining liver RNA expressions. However, further investigation is needed to address certain research gaps in this study. Firstly, we used water and ethanol as extraction solvents because dried CT is commonly consumed in food by brewing tea or infusing it in liquor. This study elucidates the mechanism of CT as a functional food against hyperglycemia caused by HFD. However, there may be more efficient methods from an industrial extraction perspective. Secondly, this article assesses HFD mice as obesity-mediated hyperglycemia, basing their increase in body weight and blood glucose criteria. It is important to note that there are differences between the two batches of mice (both were modeled as obesity-hyperglycemia) included in the experiment in terms of the HFD (either 45% for 10 weeks or 60% for 11 weeks) they were given. Finally, The scientific significance of this article is limited to the verification at the transcription level only, as it did not include the measurement of changes in protein levels. Future research could focus on determining the intervention effect of CT on hyperglycemia at the protein level, as well as its impact on mouse liver primary cells.

In conclusion, obesity resulting from excessive energy intake is often accompanied by elevated blood glucose levels and insulin

resistance. Based on *in Vivo* and *in Vitro* verification, we found that *Coreopsis tinctoria* alleviates obesity, promotes energy consumption, and improves insulin sensitivity in mice. The water extract of CT exhibited the most effective recovery effect on energy metabolism at a dose of 4 g/kg.bw. Kaempferol is the key active compound in CT. It significantly facilitates the impaired glucose consumption caused by PA treatment in L02 cells. Also, kaempferol affects carbon metabolism, glycolysis/gluconeogenesis, and MAPK signaling pathways in the liver, reducing blood sugar levels in obese mice.

Ethics statement

68 SPF grade male C57BL/6J mice was used in this experiment. All animal experiments complied with the ARRIVE guidelines. This experiment was approved by the Animal Ethics Committee of China Agricultural University (Approval number: KY1700038).

Funding

Not applicable: This experiment did not receive any funding from organization, enterprise or individual.

CRediT authorship contribution statement

Bingxin Huangfu: Writing – original draft, Software, Formal analysis, Conceptualization. **Minglan Yang:** Writing – original draft, Formal analysis, Data curation, Conceptualization. **Jia Xu:** Methodology. **Ruxin Gao:** Methodology. **Yanzhou Hu:** Data curation. **Yijia Zhao:** Methodology. **Kunlun Huang:** Writing – review & editing, Supervision. **Xiaoyun He:** Writing – review & editing, Supervision, Resources.

Declaration of competing interest

The authors declare that they have no conflict of interest or personal relationships related to the publication of this paper.

Data availability

Data will be made available on request from the authors.

Abbreviation

Abbreviation	*Full Spelling*
ALB	albumin
ALP	alkaline phosphatase
ALT	alanine aminotransferase
AST	aspartate aminotransferase
BP	biological process
BUN	blood urea nitrogen
bw	body-weight
CC	cellular component
CHO	cholesterol
CREA	creatinine
CT	*Coreopsis tinctoria*
EGFR	epidermal growth factor receptor
EH	high dose ethanol extract
EL	low dose ethanol extract
EP	epididymal fat
ESR1	estrogen receptor 1
GLU	glucose
GO	gene ontology
gtt	glucose tolerance test
HDL	high-density lipoprotein
HFD	high-fat diets
PKLR	Pyruvate kinase L/R
HSP90AA1	human heat shock protein 90 kDa alpha itt insulin tolerance test
KDR	kinase insert domain receptor
KEGG	Kyoto Encyclopedia of Genes and Genomes
LC-MS	liquid chromatography-mass spectrometry
LDL	low-density lipoprotein
MF	molecular function

NAFLD	non-alcoholic fatty liver disease
PA	sodium palmitate
PLS-DA	Partial least squares-discriminant analysis
PPI	protein-protein interaction
SD	square deviation
SRC	SRC proto-oncogene, non-receptor tyrosine kinase
SUB	subcutaneous fat
TCMSP	traditional Chinese medicine systems pharmacology database and analysis platform
TG	triglycerides
TP	total protein
UA	uric acid
WH	high dose water extract
WL	low dose water extract
PG	plasma glucose
SDSL	serine dehydratase like

Appendix A. Supplementary data

Supplementary data to this article can be found online at https://doi.org/10.1016/j.heliyon.2024.e27449.

References

[1] M.C. Wong, J. Huang, J. Wang, P.S. Chan, V. Lok, X. Chen, C. Leung, H.H. Wang, X.Q. Lao, Z.-J. Zheng, Global, regional and time-trend prevalence of central obesity: a systematic review and meta-analysis of 13.2 million subjects, Eur. J. Epidemiol. 35 (2020) 673–683.

[2] G. Gupta, R. Wadhwa, P. Pandey, S.K. Singh, M. Gulati, S. Sajita, M. Mehta, A.K. Singh, H. Dureja, T. Collet, Obesity and diabetes: pathophysiology of obesity-induced hyperglycemia and insulin resistance, Pathophysiology of obesity-induced health complications 19 (ABHD) (2020) 81–97.

[3] Z.F. Bhat, J.D. Morton, S. Mason, A.E.-D.A. Bekhit, H.F. Bhat, Obesity and neurological disorders: dietary perspective of a global menace, Crit. Rev. Food Sci. Nutr. 59 (8) (2019) 1294–1310.

[4] S. Cho, H. Lee, J. Han, H. Lee, R.O. Kattia, Z.V. Nelson, S. Choi, S.-Y. Kim, H.-Y. Park, H.G. Jeong, Viburnum stellato-tomentosum extract suppresses obesity and hyperglycemia through regulation of lipid metabolism in high-fat diet-fed mice, Molecules 26 (4) (2021) 1052.

[5] S. Shan-Shan, W. Kai, M. Ke, B. Li, L. Hong-Wei, An insoluble polysaccharide from the sclerotium of Poria cocos improves hyperglycemia, hyperlipidemia and hepatic steatosis in ob/ob mice via modulation of gut microbiota, Chin. J. Nat. Med. 17 (1) (2019) 3–14.

[6] M. Tiss, Z. Souiy, L. Achour, K. Hamden, Ephedra alata extracts exerts anti-obesity, anti-hyperglycemia, anti-antipyretic and analgesic effects, Nutr. Food Sci. 52 (1) (2022) 119–128.

[7] Q. Yu, W. Chen, J. Zhong, D. Huang, W. Shi, H. Chen, C. Yan, Purification, structural characterization, and bioactivities of a polysaccharide from Coreopsis tinctoria, Food Frontiers 3 (4) (2022) 736–748.

[8] H. Zhang, J. Zhong, Q. Zhang, D. Qing, C. Yan, Structural elucidation and bioactivities of a novel arabinogalactan from Coreopsis tinctoria, Carbohydr. Polym. 219 (2019) 219–228.

[9] J. Shen, M. Hu, W. Tan, J. Ding, B. Jiang, L. Xu, H. Hamulati, C. He, Y. Sun, P. Xiao, Traditional uses, phytochemistry, pharmacology, and toxicology of Coreopsis tinctoria Nutt.: a review, J. Ethnopharmacol. 269 (2021) 113690.

[10] L. Guo, W. Zhang, S. Li, C.-T. Ho, Chemical and nutraceutical properties of Coreopsis tinctoria, J. Funct.Foods 13 (2015) 11–20.

[11] Y. Wufuer, X. Yang, L. Guo, K. Aximujiang, L. Zhong, K. Yunusi, G. Wu, The antitumor effect and mechanism of total flavonoids from Coreopsis tinctoria nutt (snow Chrysanthemum) on lung cancer using network pharmacology and molecular docking, Front. Pharmacol. 13 (2022) 761785.

[12] H. Li, G. Xu, D. Wu, J. Li, J. Cui, J. Liu, Effects of ethyl acetate extract from Coreopsis tinctoria on learning and memory impairment in d-galactose-induced aging mice and the underlying molecular mechanism, Food Funct. 12 (6) (2021) 2531–2542.

[13] P. Ma, F. Yu, Y. Zhong, L. Xu, P. Xiao, Protective effects of flavonoids in Coreopsis tinctoria Nutt. in a mouse model of type 2 diabetes, J. Ethnopharmacol. 307 (2023) 116214.

[14] S.C. Lam, S.F. Lam, J. Zhao, S.P. Li, Rapid identification and comparison of compounds with antioxidant activity in Coreopsis tinctoria herbal tea by high-performance thin-layer chromatography coupled with DPPH bioautography and densitometry, J. Food Sci. 81 (9) (2016) C2218–C2223.

[15] D. Du, T. Jin, Z.-H. Xing, L.-Q. Hu, D. Long, S.-F. Li, M. Gong, One new linear C14 polyacetylene glucoside with antiadipogenic activities on 3T3-L1 cells from the capitula of Coreopsis tinctoria, J. Asian Nat. Prod. Res. 18 (8) (2016) 784–790.

[16] Y. Li, X. Chen, J. Xue, J. Liu, X. Chen, M. Wulasihan, Flavonoids furom Coreopsis tinctoria adjust lipid metabolism in hyperlipidemia animals by down-regulating adipose differentiation-related protein, Lipids Health Dis. 13 (1) (2014) 1–8.

[17] T. Dias, M.R. Bronze, P.J. Houghton, H. Mota-Filipe, A. Paulo, The flavonoid-rich fraction of Coreopsis tinctoria promotes glucose tolerance regain through pancreatic function recovery in streptozotocin-induced glucose-intolerant rats, J. Ethnopharmacol. 132 (2) (2010) 483–490.

[18] M. Zhang, N. Zhao, M. Xie, D. Dong, W. Chen, Y. He, D. Yan, H. Fu, X. Liang, L. Zhou, Antioxidant properties of polyphenols from snow chrysanthemum (Coreopsis tinctoria) and the modulation on intestinal microflora in vitro, Pharmaceut. Biol. 60 (1) (2022) 1771–1780.

[19] L. Rui, Energy metabolism in the liver, Compr. Physiol. 4 (1) (2014) 177.

[20] S.O. Jensen-Cody, M.J. Potthoff, Hepatokines and metabolism: deciphering communication from the liver, Mol. Metabol. 44 (2021) 101138.

[21] J.-C. Tsai, C.-S. Chiu, Y.-C. Chen, M.-s. Lee, X.-Y. Hao, M.-T. Hsieh, C.-P. Kao, W.-H. Peng, Hepatoprotective effect of Coreopsis tinctoria flowers against carbon tetrachloride-induced liver damage in mice, BMC Compl. Alternative Med. 17 (2017) 1–9.

[22] Y. Tian, Y. Li, F. Li, Q. Zhi, F. Li, Y. Tang, Y. Yang, R. Yin, J. Ming, Protective effects of Coreopsis tinctoria flowers phenolic extract against D-galactosamine/lipopolysaccharide-induced acute liver injury by up-regulation of Nrf2, PPARα, and PPARγ, Food Chem. Toxicol. 121 (2018) 404–412.

[23] J. Gao, S. Li, R. Ma, L. Shao, A. Xie, Z. Wang, Y. Zhao, Y. Li, H. Han, Protective effect of Coreopsis tinctoria nutt. Ethanol extract against acrylamide-induced liver injury, MODERN FOOD SCIENCE & TECHNOLOGY 38 (8) (2022) 17–26.

[24] B. Jiang, Q. Lv, W. Wan, L. Le, L. Xu, K. Hu, P. Xiao, Transcriptome analysis reveals the mechanism of the effect of flower tea Coreopsis tinctoria on hepatic insulin resistance, Food Funct. 9 (11) (2018) 5607–5620.

[25] F. Zhang, M. Yang, J. Xu, Y. Hu, R. Gao, K. Huang, X. He, Coreopsis tinctoria and its flavonoids ameliorate hyperglycemia in obese mice induced by high-fat diet, Nutrients 14 (6) (2022) 1160.

[26] F. Liu, N. Gao, R. Yang, Comparison of obesity models established in the different strains of mice and the mechanism of obese C57BL/6J mice, Chin. Pharmacol. Bull. 29 (3) (2013) 360–365.
[27] C. Moro, C. Magnan, GTTs and ITTs: aim for shorter fasting times, Nat. Metab. 3 (9) (2021) 1133, 1133.
[28] S. Virtue, A. Vidal-Puig, GTTs and ITTs in mice: simple tests, complex answers, Nat. Metab. 3 (7) (2021) 883–886.
[29] P.F. Pedro, A. Tsakmaki, G.A. Bewick, The glucose tolerance test in mice, Animal Models of Diabetes: Methods and Protocols (2020) 207–216.
[30] D. Al Rijjal, M.B. Wheeler, A protocol for studying glucose homeostasis and islet function in mice, STAR protocols 3 (1) (2022) 101171.
[31] Y. Zhong, J. Jin, P. Liu, Y. Song, H. Zhang, L. Sheng, H. Zhou, B. Jiang, Berberine attenuates hyperglycemia by inhibiting the hepatic glucagon pathway in diabetic mice, Oxid. Med. Cell. Longev. 2020 (2020).
[32] T. Hu, X. Yuan, G. Wei, H. Luo, H.J. Lee, W. Jin, Myricetin-induced brown adipose tissue activation prevents obesity and insulin resistance in db/db mice, Eur. J. Nutr. 57 (2018) 391–403.
[33] P. Agu, C. Afiukwa, O. Orji, E. Ezeh, I. Ofoke, C. Ogbu, E. Ugwuja, P. Aja, Molecular docking as a tool for the discovery of molecular targets of nutraceuticals in diseases management, Sci. Rep. 13 (1) (2023) 13398.
[34] Y. Ma, S. Xiang, W. Jiang, L. Kong, Z. Tan, Z. Liang, Z. Yuan, J. Yi, L. Zhu, Gamma-oryzanol protects human liver cell (L02) from hydrogen peroxide-induced oxidative damage through regulation of the MAPK/Nrf2 signaling pathways, J. Food Biochem. 46 (7) (2022) e14118.
[35] X.-L. Jin, K. Wang, Q.-Q. Li, W.-L. Tian, X.-F. Xue, L.-M. Wu, F.-L. Hu, Antioxidant and anti-inflammatory effects of Chinese propolis during palmitic acid-induced lipotoxicity in cultured hepatocytes, J. Funct.Foods 34 (2017) 216–223.
[36] X. Wan, W. Yang, Y. Xia, J. Wang, T. Lu, X. Wang, Disruption of glucose homeostasis and induction of insulin resistance by elevated free fatty acids in human L02 hepatocytes, J. Endocrinol. Invest. 32 (2009), 454-259.
[37] P. Lang, S. Hasselwander, H. Li, N. Xia, Effects of different diets used in diet-induced obesity models on insulin resistance and vascular dysfunction in C57BL/6 mice, Sci. Rep. 9 (1) (2019) 19556.
[38] N.L. Stott, J.S. Marino, High fat rodent models of type 2 diabetes: from rodent to human, Nutrients 12 (12) (2020) 3650.
[39] R. Liu, K. Chen, N. Jansz, M.E. Blewitt, M.E. Ritchie, Transcriptional profiling of the epigenetic regulator Smchd1, Genomics Data 7 (2016) 144–147.
[40] L. Li, Z. Pan, X. Yang, Key genes and co-expression network analysis in the livers of type 2 diabetes patients, Journal of diabetes investigation 10 (4) (2019) 951–962.
[41] Y.T. Wondmkun, Obesity, insulin resistance, and type 2 diabetes: associations and therapeutic implications, Diabetes, Metabolic Syndrome and Obesity (2020) 3611–3616.
[42] Y. Gu, Z.-L. Qiu, D.-Z. Liu, G.-L. Sun, Y.-C. Guan, Z.-Q. Hei, X. Li, Differential gene expression profiling of the sciatic nerve in type 1 and type 2 diabetic mice, Biomedical reports 9 (4) (2018) 291–304.
[43] A. Ullah, A. Ud Din, W. Ding, Z. Shi, S. Pervaz, B. Shen, A narrative review: CXC chemokines influence immune surveillance in obesity and obesity-related diseases: type 2 diabetes and nonalcoholic fatty liver disease, Rev. Endocr. Metab. Disord. (2023) 1–21.
[44] M. Qatanani, M.A. Lazar, Mechanisms of obesity-associated insulin resistance: many choices on the menu, Gene Dev. 21 (12) (2007) 1443–1455.
[45] A.S. Al-Goblan, M.A. Al-Alfi, M.Z. Khan, Mechanism linking diabetes mellitus and obesity, Diabetes, Metab. Syndrome Obes. Targets Ther. 7 (2014) (2014) 587–591.
[46] F. Luo, Y. Manse, S. Ishikawa, S. Nishi, A. Chen, T. Wang, T. Morikawa, Aromatase inhibitors isolated from a flowering tea, snow Chrysanthemum (the capitula of Coreopsis tinctoria Nutt.), J. Nat. Med. 77 (2023) (2023) 1–10.
[47] Y. Zhang, L. Luo, Z. Li, H. Li, X. Yao, R. Luo, Anti-lipid peroxidation, α-glucosidase and α-amylase inhibitory effects of the extract of capitula of Coreopsis tinctoria nutt. And protection effects on high-fat/high-sugar and streptozotocin-induced type 2 diabetes in mice, Chem. Biodivers. 16 (12) (2019) e1900514.
[48] K.Y. Chen, R.J. Brychta, Z.A. Sater, T.M. Cassimatis, C. Cero, L.A. Fletcher, N.S. Israni, J.W. Johnson, H.J. Lea, J.D. Linderman, Opportunities and challenges in the therapeutic activation of human energy expenditure and thermogenesis to manage obesity, J. Biol. Chem. 295 (7) (2020) 1926–1942.
[49] Z. Gao, J. Yin, J. Zhang, R.E. Ward, R.J. Martin, M. Lefevre, W.T. Cefalu, J. Ye, Butyrate improves insulin sensitivity and increases energy expenditure in mice, Diabetes 58 (7) (2009) 1509–1517.
[50] C. Depommier, M. Van Hul, A. Everard, N.M. Delzenne, W.M. De Vos, P.D. Cani, Pasteurized Akkermansia muciniphila increases whole-body energy expenditure and fecal energy excretion in diet-induced obese mice, Gut Microb. 11 (5) (2020) 1231–1245.
[51] T. Zou, S. Li, B. Wang, Z. Wang, Y. Liu, J. You, Curcumin improves insulin sensitivity and increases energy expenditure in high-fat-diet–induced obese mice associated with activation of FNDC5/irisin, Nutrition 90 (2021) 111263.
[52] Y. Xu, Y. Lou, J. Kong, VDR regulates energy metabolism by modulating remodeling in adipose tissue, Eur. J. Pharmacol. 865 (2019) 172761.
[53] W. Xin, W. Zi-Yi, J.-H. Zheng, L. Shao, TCM network pharmacology: a new trend towards combining computational, experimental and clinical approaches, Chin. J. Nat. Med. 19 (1) (2021) 1–11.
[54] M. Zhang, X. Zhang, The role of PI3K/AKT/FOXO signaling in psoriasis, Arch. Dermatol. Res. 311 (2019) 83–91.
[55] A.E.G. Whitlock, J. Sostre-Colón, M. Gavin, N.D. Martin, J.A. Baur, C.A. Sims, P.M. Titchenell, Loss of FOXO transcription factors in the liver mitigates stress-induced hyperglycemia, Mol. Metabol. 51 (2021) 101246.
[56] Y. Ballestero, J. López-Herce, R. González, M.J. Solana, J. Del Castillo, J. Urbano, M. Botran, A. García, N. López, J.M. Bellón, Relationship between hyperglycemia, hormone disturbances, and clinical evolution in severely hyperglycemic post surgery critically ill children: an observational study, BMC Endocr. Disord. 14 (1) (2014) 1–8.
[57] J.N. Lo Cascio, A. Jordan, M.F. Anderman, B.D. Shepard, Modulation of estrogen receptor signaling sensitizes female mice to the development of diabetes, Faseb. J. 36 (2022).
[58] J. Liu, Y. Lin, C. Peng, C. Jiang, J. Li, W. Wang, S. Luo, P. Fu, Z. Lin, Y. Liang, Bisphenol F induced hyperglycemia via activation of oxidative stress-responsive miR-200 family in the pancreas, Ecotoxicol. Environ. Saf. 255 (2023) 114769.
[59] E. Jing, P. Sundararajan, I.D. Majumdar, S. Hazarika, S. Fowler, A. Szeto, S. Gesta, A.J. Mendez, V.K. Vishnudas, R. Sarangarajan, Hsp90β knockdown in DIO mice reverses insulin resistance and improves glucose tolerance, Nutr. Metabol. 15 (2018) 1–10.
[60] P. Ahuja, X. Bi, C.F. Ng, M.C.L. Tse, M. Hang, B.P.S. Pang, E.C.Y. Iu, W.S. Chan, X.C. Ooi, A. Sun, Src homology 3 domain binding kinase 1 protects against hepatic steatosis and insulin resistance through the Nur77–FGF21 pathway, Hepatology 77 (1) (2022) 213–229.
[61] Z. Chen, D. Tian, X. Liao, Y. Zhang, J. Xiao, W. Chen, Q. Liu, Y. Chen, D. Li, L. Zhu, Apigenin combined with gefitinib blocks autophagy flux and induces apoptotic cell death through inhibition of HIF-1α, c-Myc, p-EGFR, and glucose metabolism in EGFR L858R+ T790M-mutated H1975 cells, Front. Pharmacol. 10 (2019) 260.
[62] L. Liu, S. Sun, X. Li, A network pharmacology-based approach to explore the effect of dihydromyricetin on non-alcoholic fatty liver rats via regulating PPARG and CASP3, Mol. Cell. Probes 71 (2023) 101926.
[63] A.R. Devan, B. Nair, A.R. Kumar, L.R. Nath, An insight into the role of telmisartan as PPAR-γ/α dual activator in the management of nonalcoholic fatty liver disease, Biotechnol. Appl. Biochem. 69 (2) (2022) 461–468.
[64] R.J. Perry, V.T. Samuel, K.F. Petersen, G.I. Shulman, The role of hepatic lipids in hepatic insulin resistance and type 2 diabetes, Nature 510 (7503) (2014) 84–91.
[65] S. Parekh, F.A. Anania, Abnormal lipid and glucose metabolism in obesity: implications for nonalcoholic fatty liver disease, Gastroenterology 132 (6) (2007) 2191–2207.
[66] KEGG PATHWAY: hsa01200. https://www.genome.jp/dbget-bin/www_bget?pathway+hsa01200 (accessed 29).

[67] L. Agius, B.E. Ford, S.S. Chachra, The metformin mechanism on gluconeogenesis and AMPK activation: the metabolite perspective, Int. J. Mol. Sci. 21 (9) (2020) 3240.
[68] X. Chen, Y.-l. Tong, Z.-m. Ren, S.-s. Chen, X.-y. Mei, Q.-y. Zhou, G.-h. Dai, Hypoglycemic mechanisms of Polygonatum sibiricum polysaccharide in db/db mice via regulation of glycolysis/gluconeogenesis pathway and alteration of gut microbiota, Heliyon 9 (4) (2023) e15278.
[69] X. Wen, B. Zhang, B. Wu, H. Xiao, Z. Li, R. Li, X. Xu, T. Li, Signaling pathways in obesity: mechanisms and therapeutic interventions, Signal Transduct. Targeted Ther. 7 (1) (2022) 298.